PLANKTONIC FORAM DATES FROM THE INDONESIAN ARC: MARINE ^{14}C RESERVOIR AGES AND A MYTHICAL AD 535 ERUPTION OF KRAKATAU

John Southon[1] • Mahyar Mohtadi[2] • Ricardo De Pol-Holz[3]

ABSTRACT. The Indonesian Arc represents the subduction of the Indian-Australian plate beneath Asia. It has been the scene of catastrophic tectonic activity, including the recent 2004 M=9.1 Aceh earthquake and resulting Indian Ocean tsunami. We have dated planktonic forams associated with historic tephras (Tambora, 1815 and Krakatau, 1883) in marine sediment cores to determine radiocarbon reservoir ages for 2 locations along the arc. Our best estimates for 19th century regional reservoir corrections (ΔR) are +90 ± 40 yr for surface-dwelling species and +220 ± 40 yr for mixed planktic assemblages containing some upper thermocline species, but scatter in the data suggests that past surface reservoir ages may have varied by about ±100 yr. We used the results of this study to investigate a proposed very large AD 535 eruption at or near Krakatau. We find no evidence for ash from such an eruption, and although this is negative evidence, we consider it sufficiently strong to rule out any possibility that one took place.

INTRODUCTION

The Indonesian Arc extends 6000 km from the Andaman Islands in the Bay of Bengal to the Banda Sea south of western New Guinea, and was formed by the subduction of the Indian-Australian plate beneath Asia. The resulting violent tectonic activity has included numerous large volcanic and seismic events (Newcomb and McGann 1987; Simkin and Siebert 1994), some involving tens to hundreds of thousands of fatalities and catastrophic damage to infrastructure. These disasters include the 1815 VEI (Volcanic Explosivity Index) 7 eruption of Mount Tambora in the Lesser Sunda Islands east of Java (Self et al. 1984), the 1883 VEI 6 eruption of Krakatau in Sunda Strait between Java and Sumatra (Verbeek 1885), and the 26 December 2004 M=9.1 Aceh earthquake off northern Sumatra and the resulting Indian Ocean tsunami (Lay et al. 2005).

The effects of large subduction-related earthquakes and volcanic eruptions are recorded as turbidites and ash layers in marine sediment records from the south side of the arc. These sedimentary archives also monitor the state of the Indonesian Throughflow (ITF), a critical choke point in the surface return path of the Global Ocean Conveyor Circulation (Broecker 1991); they are therefore of interest to paleoceanographers, tectonicists, and paleoseismologists alike. The present study is aimed at improving radiocarbon chronologies for such sediments by providing regional marine ^{14}C reservoir ages determined from ^{14}C dates on planktic foraminifera, using tephra layers from known-age volcanic eruptions as time markers.

METHODS

The core locations for the study (Figure 1) all lie within the domain of the seasonally reversing (monsoon driven) South Java Current that runs along the south side of the Sunda Arc. The near-surface hydrography of this region is subject to strong seasonal forcing from heavy precipitation and the southward advection of low-salinity Java Sea water during the northwest monsoon (Wijffels et al. 1996; Sprintall et al. 2003; Mohtadi et al. 2009), and the upwelling of subsurface water in the region south of Java during the southeast monsoon (Susanto et al. 2001). These annual cycles are

[1]Earth System Science Department, University of California, Irvine, California 92697, USA. Corresponding author. Email: jsouthon@uci.edu.
[2]MARUM, University of Bremen, Loebener Str., 28359 Bremen, Germany.
[3]Department of Oceanography, Universidad de Concepción, Casilla 160-C, Concepción, Chile.

Proceedings of the 21st International Radiocarbon Conference edited by A J T Jull & C Hatté
RADIOCARBON, Vol 55, Nr 2–3, 2013, p 1164–1172

strongly modulated on interannual and longer timescales by ENSO and its Indian Ocean equivalent, the Indian Ocean Dipole (IOD). Positive IOD events are associated with strong cooling and enhanced upwelling off Sumatra (Abram et al. 2007), while El Niño events are associated with severe droughts in Sumatra and Java and weakened ITF flow, which influences both thermocline and sea surface temperatures in the South Java Current (Susanto et al. 2001).

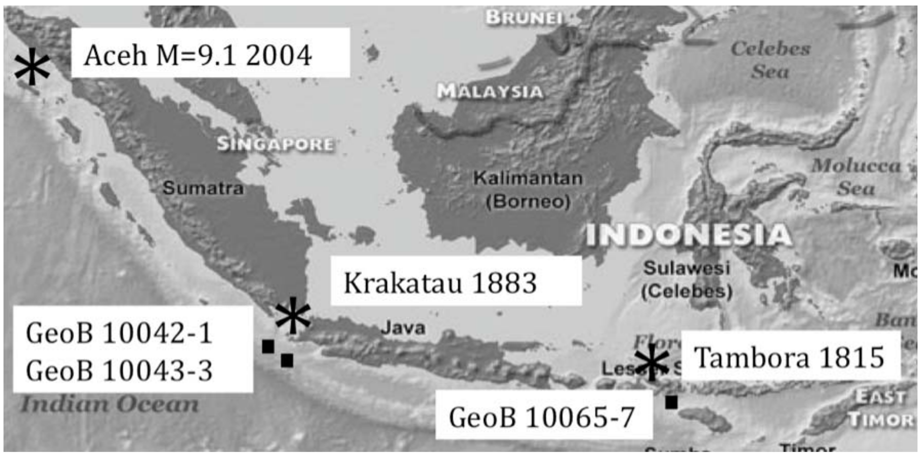

Figure 1 Map of Indonesia, showing the locations of the 1815 Tambora and 1883 Krakatau eruptions and the 2004 Aceh earthquake, plus sampling locations for marine sediment cores used in this study.

Gravity cores GeoB 10042-1 (7°06.81′S 104°38.58′E, 2454 m water depth) and GeoB 10043-3 (7°18.57′S 105°3.53′E, 2171 m) were recovered on the 2005 SO184-2 cruise of the German R/V *Sonne*, from locations southwest of the Sunda Strait separating Java and Sumatra. GeoB 10065-7 (9°13.39′S 118°53.58′E, 1296 m) was collected in the strait between Sumba and Sumbawa in the Lesser Sunda Islands east of Java, on the same cruise (Figure 1). The major lithologies for all 3 cores are characterized in SO184-2 core logs as olive to olive gray foraminifera, and diatom-bearing nanofossil ooze. None of the cores is anoxic, but the core logs record that portions of GeoB 10065-7 smelt of H_2S, and GeoB 10042-1 and 10043-3 are characterized as moderately and weakly bioturbated, respectively, suggesting that bioturbational mixing is of minor importance within these low-oxic sediments, particularly when sedimentation rates are high.

All 3 cores contain visually prominent layers of volcanic ash within a few cm or tens of cm of the sediment surface. Historical records of volcanism around Sunda Strait and in the Lesser Sunda Islands (Simkin and Siebert 1994) show only modest activity for several centuries prior to the 1883 Krakatau and 1815 Tambora events. Apart from the 1822 VEI 5 eruption of Galunggung 300 km east of Sunda Strait, which produced ash fall extending no more than ~40 km from the volcano itself (Bronto 1989), all 19th century eruptions within ~600 km of the GeoB core sites were VEI 3 or less and could not have produced heavy ash fall at these locations. The thick ash layers near the core tops of GeoB 10042-1 and 10043-3, and of GeoB 10065-7, can therefore be unambiguously associated with the very large Krakatau and Tambora eruptions, respectively.

Visual and X-ray fluorescence studies of the GeoB 10065-7 ash showed that the single ash layer reported in the SO 184-2 cruise log is in fact a doublet, consisting of a thick upper layer at 37–40 cm core depth and a lower layer at 45–46 cm. The upper surfaces of both layers grade into the overlying greenish sediments due to postdepositional bioturbation, indicating that the intervening 5 cm of sediment was deposited *in situ* and represents an interval of at least several decades prior to the Tambora eruption. The lower ash probably originated from an 18th century eruption in the Lesser Sunda Islands, where documentation of volcanic activity prior to 1800 is sparse (Simkin and Siebert 1994).

Comparison with ^{210}Pb-dated multicores from the GeoB 10065 site (S Steinke, personal communication) shows that 10 cm of surface sediment is missing from the gravity core and that a depth of 35 cm in GeoB 10065-7 corresponds to AD 1859 in the ^{210}Pb chronology. The 36-cm depth just above the Tambora layer in GeoB 10065-7 therefore corresponds to a calendar age between 1855 and 1817, depending on whether we extrapolate the ^{210}Pb chronology or derive an age based on the average post-eruption sedimentation rate of (37 + 10) cm/190 yr, and we take the calendar age as AD 1835 ± 20.

Sediment deposition immediately below the 1883 Krakatau ash in GeoB 10043-3 was a modest 10 cm/kyr (Figure 3), so that a 1-cm depth increment spans ~100 yr, and we adopt an age of AD 1835 ± 50 for the calendar age range of the samples from 18 cm in that core. Sedimentation rates have increased markedly since the Krakatau eruption, both in that core and in 10042-1 (see below). If we assume that this increase was linear with time, starting from a base rate of 10 cm/kyr in both cores, the ages for the 1-cm layers just above the ash, centered on 6 cm in GeoB 10042-1 and 13 cm in GeoB 10043-3, are AD 1905 ± 20 and 1895 ± 10, respectively.

Foraminifera for ^{14}C dating were picked from the >250-μm fraction of sieved sediment samples spanning 1 cm of core depth. They were cleaned by brief sonication in methanol and subsequently by removal of 10% of the carbonate with 0.01N HCl, prior to hydrolysis with H_3PO_4, conversion to graphite, and measurement by accelerator mass spectrometry (AMS). Surface-dwelling species *G. sacculifer* (without the final sac-like chamber) and *G. ruber sensu stricto* (s.s.) were selected for dating as best representing ^{14}C within the ocean mixed layer. However, the concentrations of these species within the cores were generally low, and it was sometimes necessary to use combined samples to obtain sufficient weight. Furthermore, since core chronologies in future studies may be based on mixed planktic assemblages that include some upper thermocline species, we also measured mixed samples (more precisely, "residual assemblage" samples), consisting of the planktic forams remaining in the >250-μm fraction after the *G. sacculifer* and *G. ruber* tests had been picked. These residuals typically represented 70–90% of the total mass of >250-μm planktics and hence approximated true mixed planktic assemblages. The most common species in these samples included *G. bulloides*, which inhabits the lower mixed layer, plus *N. pachyderma dex.*, *N. dutertrei*, *G. menardii*, and *G. inflata*, which calcify in the upper thermocline (Mohtadi et al. 2011). Samples in and around the ash layers in all 3 cores were dated, plus additional samples from the top 50 cm of GeoB 10042-1 and 10043-3.

RESULTS

The ^{14}C results are summarized in Table 1, and data from GeoB 10042-1 and 10043-3 are plotted in Figures 2 and 3, respectively. ^{14}C age uncertainties for the larger samples in Table 1 are typically ±15 to 25 yr (1σ): increased uncertainties on some monospecific and combined *G. ruber* + *G. sacculifer* samples are due to very small sample sizes. Regional reservoir corrections (ΔR) were calculated as differences between the measured ^{14}C ages and the predictions of the Marine09 global marine ^{14}C model (Reimer et al. 2009) for the same calendar ages. For cases where the 1-cm sediment samples spanned several decades or the actual calendar age was uncertain, the resulting additional uncertainty in the model reservoir ages *R* was added in quadrature with the quoted error in *R* (Reimer et al. 2009) and the analytical ^{14}C error in determining the ΔR uncertainty.

Table 1 Radiocarbon results from this study.

UCIAMS #	Depth (cm)	Species[a]	Size (mg C)[b]	^{14}C age (BP)	Calendar age[c]	Model *R*	ΔR (^{14}C yr)
Core GeoB 10042-1 (7°6.81′S, 104°38.58′E, 2454 m)							
98273	3	Mixed pl.	0.054	105 ± 25			Bomb ^{14}C
89144	6	*Ruber+Sacc*.	0.083	515 ± 20	1905 ± 20	460 ± 25	55 ± 35
Ash 6–8 cm (Krakatau, 1883)							
89145	8	*Ruber+Sacc*.	0.13	3895 ± 20			Missing core
98274	8	Mixed pl.	0.10	4170 ± 20			
98275	13	Mixed pl.	0.29	4360 ± 15			
98276	13	*Sacculifer*	0.069	4225 ± 40			
98277	18	Mixed pl.	0.42	4500 ± 15			
98279	18	*Sacculifer*	0.054	4440 ± 50			
98280	23	Mixed pl.	0.79	4580 ± 15			
98281	23	*Sacculifer*	0.033	4580 ± 90			
98282	28	Mixed pl.	0.15	4815 ± 20			
98283	33	Mixed pl.	0.36	4865 ± 15			
98284	33	*Sacculifer*	0.058	4675 ± 45			
98286	33	*Ruber*	0.027	4820 ± 100			
98287	38	Mixed pl.	0.58	4975 ± 20			
98288	38	*Sacculifer*	0.26	4885 ± 20			
98289	38	*Ruber*	0.046	4930 ± 60			
98290	43	Mixed pl.	0.48	5045 ± 20			
98291	43	*Sacculifer*	0.11	5015 ± 25			
Core GeoB 10043-3 (7°18.57′S, 105°3.53′E, 2171 m)							
89142	13	*Ruber+Sacc*.	0.033	545 ± 35	1895 ± 10	460 ± 25	85 ± 45
98497	13	Mixed pl.	0.12	705 ± 15	1895 ± 10	460 ± 25	245 ± 30
Ash 13–18 cm (Krakatau, 1883)							
89143	18	*Ruber+Sacc*.	0.040	640 ± 35	1835 ± 50	505 ± 45	135 ± 60
98498	18	Mixed pl.	0.78	925 ± 15	1835 ± 50	505 ± 45	420 ± 45
98499	18	*Sacculifer*	0.15	800 ± 20	1835 ± 50	505 ± 45	295 ± 50
98500	18	*Ruber*	0.015	940 ± 80	1835 ± 50	505 ± 45	435 ± 85
98501	23	Mixed pl.	0.56	1410 ± 15			
98502	23	*Sacculifer*	0.092	1150 ± 25			
98505	28	Mixed pl.	0.44	1820 ± 15			
98506	28	*Ruber*	0.065	1570 ± 25			
98507	33	Mixed pl.	0.46	2130 ± 15			
98508	33	*Sacculifer*	0.058	2070 ± 25			
98509	38	Mixed pl.	0.64	2430 ± 20			
98510	38	*Sacculifer*	0.23	2240 ± 15			
98511	38	*Ruber*	0.017	2380 ± 80			
98517	43	Mixed pl.	0.52	2700 ± 15			
98518	43	*Sacculifer*	0.060	2525 ± 30			
98519	48	Mixed pl.	0.43	2845 ± 20			
98520	48	*Sacculifer*	0.048	2760 ± 30			
Core GeoB 10065-7 (9°13.39′S, 118°53.58′E, 1296 m)							
89139	36	*Ruber+Sacc*.	0.15	630 ± 20	1835 ± 20	500 ± 30	130 ± 35
Ash 37–40 cm (Tambora, 1815)							
89140	39[d]	*Ruber+Sacc*.	0.038	745 ± 35	1815 ± 5	520 ± 25	225 ± 45
89141	40	*Ruber+Sacc*.	0.16	1500 ± 20	1810 ± 5	525 ± 25	Reworked
84721	41	Mixed pl.	0.46	755 ± 20	1805 ± 5	535 ± 25	220 ± 30

[a]Mixed pl. = mixed planktics (residuals after *Ruber* and *Sacculifer* picked - see text); [b]Size in mg of carbon; [c]Assumed calendar age ranges for 1-cm layers centered on the depths shown (see text); [d]In ash.

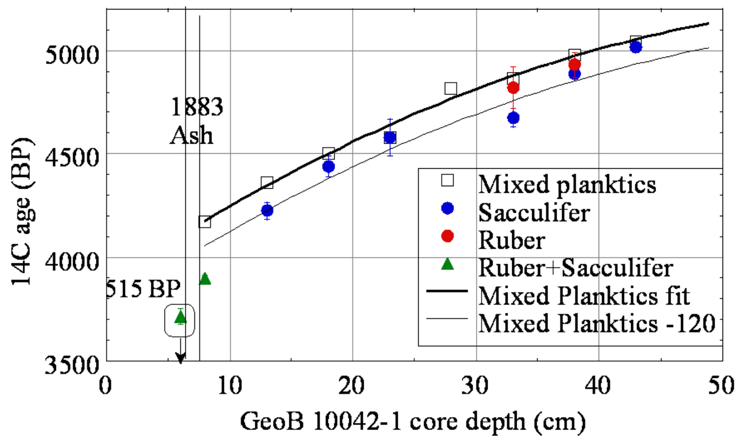

Figure 2 Radiocarbon results for core GeoB 10042-1. The thick line shows a quadratic fit to the results on mixed planktonic samples, and the quality of the fit suggests that most changes in sedimentation rate were smooth rather than abrupt. Results on monospecific and combined (*G. ruber* + *G. sacculifer*) samples show much more scatter, but are fit reasonably well by the same trend offset 120 yr to younger ages (thin line).

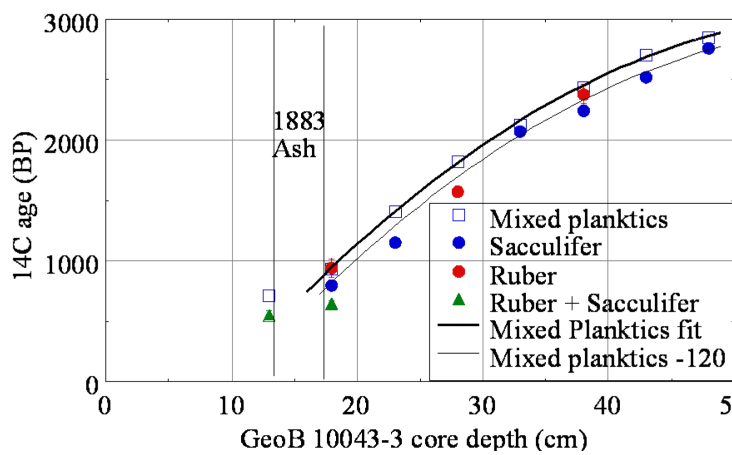

Figure 3 Radiocarbon results for core GeoB 10043-3 (see Figure 2 caption for details)

The very young ^{14}C age for the 3-cm sample from GeoB 10042-1 shows that this sample is contaminated with bomb ^{14}C. We cannot completely exclude the possibility that bomb carbon has also been bioturbated down into the 6-cm *G. ruber* + *G. sacculifer* sample from this core, but this result is consistent with the corresponding sample in GeoB 10043-3, where the higher sedimentation rate rules out any bomb ^{14}C influence. Ages in GeoB 10042-1 below the Krakatau ash increase abruptly to ~4000 BP, indicating that a large section of sediment is missing from the record. In GeoB 10043-3, ages below the Krakatau ash are also older than those above; but only by 100–200 yr (excluding 1 result on a very small *G. ruber* sample). This offset may be due to differential effects of bioturbation on samples above and below the ash layer, which would bias the upper and lower samples younger and older, respectively; or possibly to minor erosion of the sediment surface as the ash was deposited. A very old *G. ruber* + *G. sacculifer* result from 40 cm in GeoB 10065-7 suggests that the base of the 37–40 cm Tambora ash layer incorporated some old sediment, though ages for a mixed planktic sample at 41 cm and a *G. ruber* + *G. sacculifer* sample at 39 cm (within the ash itself) both appear reasonable. Downcore ages for (*G. ruber* + *G. sacculifer*) samples in GeoB 10042-1 and 10043-3 are 0–300 yr younger, and significantly more scattered, than those for mixed planktics, but the mixed vs. *G. ruber* and *G. sacculifer* age differences are consistent with a ~120-yr offset in both cores (Figures 2 and 3).

DISCUSSION

ΔR Values

In view of the possibly erosive nature of the ash deposition process (particularly for GeoB 10065-7), we take the ^{14}C results from just above the ash layers as the most reliable for determining recent ΔR values. ^{14}C dates on combined *G. ruber* + *G. sacculifer* samples require regional reservoir corrections (ΔR) ranging from +55 to +130 ^{14}C yr, and a single mixed planktic result from GeoB 10043-3 yields ΔR = +245 yr. Downcore ages for *G. ruber* and *G. sacculifer* samples show substantial scatter (up to ±150 yr) about a long-term trend, consistent with the strong ENSO- and IOD-induced variability on interannual and longer timescales that appears in near-surface hydrography (Sprintall et al. 2003; Mohtadi et al. 2009). Mixed planktonics require an additional correction of 100–150 yr relative to the surface dwellers: this additional ^{14}C depletion in the deeper dwelling species is consistent with the upwelling of subsurface waters off Java and Sumatra (Susanto et al. 2001), and their subsequent east-west distribution by the seasonally reversing South Java Current. Results on these species exhibit notably smaller scatter than those of the mixed layer species, probably due to the attenuation of the effects of changes in atmospheric forcing in the thermocline.

The data for combined *G. ruber* + *G. sacculifer* samples from above the dated ash layers give a mean ΔR of +90 ± 40 yr, but the scatter in the downcore data from those surface species suggests that the real ΔR variability due to hydrographic variations forced by ENSO-, IOD-, and monsoon-related changes could be much greater. A further potential complication arises from comparisons of *G. ruber* and *G. sacculifer* ages: 4 depth horizons from GeoB 10042-1 and 10043-3 contained sufficient numbers of both species to directly compare the ^{14}C ages on monospecific samples. Surprisingly, all 4 comparisons yielded older ^{14}C ages for *G. ruber*, though the significance is questionable given the small *G. ruber* sample sizes and resulting large uncertainties (Table 1). Both species inhabit the uppermost 20–50 m of the water column (Mohtadi et al. 2011), and while some planktonic species migrate into the thermocline near the end of their life cycle, *G. ruber* do not (Schmidt et al. 2008). A sediment trap study south of Java (Mohtadi et al. 2009) showed *G. ruber* abundance peaks extending further into the upwelling season than those of *G. sacculifer*. Hence, if the interspecies ^{14}C offset is real, it may reflect a closer coupling between blooms of *G. ruber* and the periods of strongest upwelling and maximum ^{14}C depletion at the surface.

The mixed planktic sample from above the AD 1883 ash in GeoB 10043-3 yielded a ΔR of +245 ± 30 yr, but recall that the mixed assemblages measured here were residual planktics remaining after *G. ruber* and *G. sacculifer* were picked, and typically represented (80 ± 10)% of the total mass of planktics (Table 1). Detailed comparisons of mixed vs. surface dweller ^{14}C ages from individual depth horizons within the 2 Sunda Strait cores (Table 1) give a mean age offset of 120 ± 95 yr. We therefore applied a correction of (20 ± 10)% of this mixed vs surface dweller difference to correct for any old bias resulting from over-representation of thermocline species. Our best estimate for the ΔR for true mixed assemblage samples that include all planktic species is therefore 245 ± 30 minus 25 ± 25 yr, or +220 ± 40 yr. This value is subject to significant additional uncertainty depending on the composition of the mixed assemblages sampled, and possible changes in regional upwelling strength, but the small scatter in the Sunda Strait mixed assemblage data about smooth long-term trend lines extending back several thousand years (Figures 2 and 3) argues against any large abrupt changes over that period.

The surface ΔR value of +90 ± 40 yr is significantly lower than those from other tropical/subtropical eastern boundary upwelling areas, which range as high as 250–350 yr (Berger et al. 1966; Ingram and Southon 1996; Jones et al. 2007; Ortlieb et al. 2011; see http://calib.qub.ac.uk/marine for a database of ΔR values). Together with the large and variable ^{14}C age offset of 120 ± 95 yr between surface and lower mixed layer/upper thermocline foraminifera, this argues for a partial decoupling of the surface from the effects of upwelling induced by along-shore southeast monsoon winds. Similarly, regional surface temperatures during the upwelling season show no large-scale decreases eastward from the open Indian Ocean towards the upwelling source areas off the Indonesian coast, though thermocline temperatures do drop significantly. This lack of surface temperature depression is attributed to seasonal increases in the advection of warm and relatively fresh near-surface ITF water southward through the Indonesian Archipelago, increasing stratification and deepening the thermocline south of Java, and contributing significantly to the upwelled waters that actually reach the surface (Susanto et al. 2001). Since the ITF waters originate from shallow depths in the Western Pacific Warm Pool, a non-upwelling area characterized by low ΔR values (see http://calib.qub.ac.uk/marine), this same mixing mechanism explains the low surface ΔR value derived above; and given the sensitivity of both upwelling and ITF strengths to changes in ENSO, IOD, and the monsoon, it also suggests a mechanism for much of the observed scatter in the downcore surface planktic ^{14}C ages.

Hiatus in GeoB 10042-1

The abrupt jump in ^{14}C ages in GeoB 10042-1 from 515 BP above the Krakatau ash to ~3900 BP immediately below (Figure 2), indicates that ~1 m of sediment is missing, probably due to seismically induced slumping during the 1883 eruption itself (before the major ash fall), or years to decades earlier. No major historical Indonesian earthquakes recorded before 1883 were centered near Sunda Strait, and severe shaking from the 1875 Central Java event probably did not extend as far west as the core site (Newcomb and McGann 1987). Seismicity associated with the 1883 eruption was only moderate, but the slump may be attributable to a local earthquake in 1880, which was strong enough to cause severe damage to the lighthouse on Java's First Point at the southern end of the strait (Verbeek 1885).

Sedimentation Rates

The 3 cores all exhibit very high recent sedimentation rates. The 1883 tephra layer is found at 13–18 cm in GeoB 10043-3 and at 6–8 cm in GeoB 10042-2, implying post-1883 sedimentation rates of 100 cm/kyr and 50 cm/kyr, respectively. Beauregard (2001) described a tephra layer at 23–24 cm depth in Core BAR9443 west of Sunda Strait (6°29′S 104°19′E, 2180 m water depth) that was compositionally similar to 1883 Krakatau airfall deposits, but rejected the association due to the required sedimentation rate of 180 cm/kyr, which appeared inconsistent with the presence of exposed 1883 deposits within Sunda Strait itself. Likewise, the Tambora-associated layer in core GeoB 10065-7 is at 37–40 cm: allowing for 10 cm of missing core top (see above), this requires a remarkable post-eruption sedimentation rate of 250 cm/kyr.

These exceptional sedimentation rates (and the high pre-eruption rates of up to 30–45 cm/kyr in GeoB 10042-1 and 10043-3; Figures 2 and 3) can be attributed to terrestrial runoff, with very heavy precipitation during the northwest monsoon leading to high fluvial sediment discharge. Seasonally low salinities and very high sediment trap fluxes in the South Java Current (Wijffels et al. 1996; Sprintall et al. 2003; Mohtadi et al. 2009) attest to the importance of local runoff from western

Sumatra and Java and other islands along the arc, augmented by southward advection of fresh sediment-laden waters from the Java Sea. The recent extreme sedimentation rates suggest an increasing regional impact of agriculture, logging, and other human disturbances over the past 200 yr, consistent with other evidence. Soil erosion on Java was recognized as a significant problem as early as the 1860s (Whitten et al. 1996). AVHRR satellite imagery shows numerous fluvial sediment plumes along the Java Sea coasts of Sumatra, Java, and Kalimantan (Gupta 1996), and similarly high recent sedimentation rates are observed in the eastern Java Sea near Makassar Strait (Newton et al. 2006; Oppo et al. 2009). The apparent paradox of minimal post-1883 sedimentation within Sunda Strait (Beauregard 2001) probably reflects the strong currents within the strait that inhibit deposition, preserving the Java Sea sediment load for subsequent deposition in locations further south.

Krakatau AD 535—The Eruption That Wasn't

Prior to AD 1883, GeoB 10043-3 presents an unbroken sequence of sediment for at least 2000 yr, providing an opportunity to test for the presence of tephra from a proposed very large AD 535 eruption of either Krakatau or another (as yet undiscovered) volcano in Sunda Strait. Keys (1999) and Wohletz (2000) have claimed that this was the source of a historically documented AD 536 dust veil event and subsequent decadal cooling, similar to the 1816 "year without a summer" that followed Tambora, but much more severe and prolonged (Stothers 1984; Larsen et al. 2008). Taking reservoir corrections into account, AD 535 corresponds to a depth of ~33 cm in GeoB 10043-3, but the first ash below the 1883 tephra in this core is at 225–232 cm. Hence, although GeoB 10043-3 contains a clearly visible ~5-cm-thick ash layer from the 1883 Krakatau eruption, there is no evidence for an AD 535 event, which supposedly involved tephra volumes many times larger. We discount the possibility that a significant ash layer was deposited but was removed in its entirety by slumping, erosion, or other disturbance, because such an event must also have involved sediment loss and would have interrupted the smooth age-depth trend of the GeoB 10043-3 mixed planktic dates (Figure 3).

The occurrence of a major Sunda Strait eruption without tephra deposition 130 km southwest of the source would require extraordinary meteorological conditions, as easterly winds near Sunda Strait persist throughout the year at many altitudes, with seasonal (monsoon) wind reversals only occurring below 5 km and near the tropopause (Beauregard 2001: Figures 2-22 and 2-23). Hence, the likelihood of southwesterly dispersal of ash is high, particularly for very large eruption columns that penetrate well into the stratosphere. Furthermore, ash from large eruptions is typically widely distributed about the source vent regardless of wind direction. For example, the major dispersal axes for 1883 Krakatau ash were northwest into Sumatra and southwest into the Indian Ocean, but 5 mm of tephra were deposited at Batavia 150 km east of Krakatau and ash fall was also reported at Noordwachter Island 150 km to the northeast (Verbeek 1885). Thus, for a proposed Sunda Strait eruption many times larger than the 1883 event, the absence of significant tephra deposition in a well-dated core just 130 km downwind seems so improbable that it effectively rules out any possibility that such an eruption took place. We therefore conclude that while the AD 536 dust veil event and subsequent cooling are well documented historically and in ice-core and dendro records, and were almost certainly due to explosive volcanism (Stothers 1984; Larsen 2008), the proposed large-scale AD 535 eruption of Krakatau is a myth.

ACKNOWLEDGMENTS

We thank the crew of the R/V *Sonne* for their assistance during the SO-184-2 cruise, the Bundesministerium fur Bildung und Forschung (project Pabesia) for funding the cruise, and Stephan Steinke for helpful discussions and for providing unpublished ^{210}Pb data.

REFERENCES

Abram NJ, Gagan MK, Liu Z, Hantoro WS, McCulloch MT, Surwargadi BW. 2007. Seasonal characteristic of the Indian Ocean Dipole during the Holocene epoch. *Nature* 445(7125):299–302.

Beauregard JL. 2001. Explosive rhyodacitic volcanism: the evolution and frequency of pre-1883 eruptions at Krakatau volcano, Indonesia [PhD dissertation]. University of Rhode Island. 379 p.

Berger R, Taylor RE, Libby WF. 1966. Radiocarbon content of marine shells form the California and Mexican west coast. *Science* 153(3738):864–6.

Broecker WS. 1991. The great ocean conveyor. *Oceanography* 4:79–89.

Bronto S. 1989. Volcanic geology of Galunggung, West Java, Indonesia [PhD dissertation]. University of Canterbury. 490 p.

Gupta A. 1996. Erosion and sediment yield in Southeast Asia: a regional perspective. In: Walling DE, Webb BW, editors. *Erosion and Sediment Yield: Global and Regional Perspectives*. Proceedings of the Exeter Symposium, July 1996. International Association for Hydrological Sciences Publication no. 236. p 215–22.

Ingram BL, Southon JR. 1996. Reservoir ages in eastern Pacific coastal and estuarine waters. *Radiocarbon* 38(3):573–82.

Jones KB, Hodgins GL, Dettman DL, Andrus CT, Nelson A, Etayo-Cadavid MF. 2007. Seasonal variations in Peruvian marine reservoir age from pre-bomb *Argopecten purpuratus* shell carbonate. *Radiocarbon* 49(2):877–88.

Keys D. 1999. *Catastrophe: An Investigation into the Origins of the Modern World*. New York: Ballantine. 368 p.

Larsen LB, Vinther BM, Briffa KR, Melvin TM, Clausen HB, Jones PD, Siggard-Andersen M-L, Hammer CU, Eronen M, Grudd H, Gunnarson BE, Hantemirov RM, Naurzbaev MM, Nicolussi K. 2008. New ice core evidence for a volcanic cause for the AD 536 dust veil. *Geophysical Research Letters* 35: L04708, doi: 10.1029/2007GL032450.

Lay T, Kanamori H, Ammon CJ, Nettles M, Ward SN, Aster RC, Beck SL, Bilek SL, Brudzinski MR, Butler R, DeShon HR, Ekstrom G, Satake K, Sipkin S. 2005. The great Sumatra-Andaman earthquake of 26 December 2004. *Science* 308(5725):1127–33.

Mohtadi M, Steinke S, Groenveld J, Fink HG, Rixen T, Hebblen D, Donner B, Herunadi B. 2009. Low latitude control and seasonal and interannual changes in planktonic foraminiferal flux and shell geochemistry off south Java. *Paleoceanography* 24: PA1201, doi: 10.1029/2008PA001636.

Mohtadi M, Oppo DW, Luckge A, De Pol-Holz R, Steinke S, Groeneveld J, Hemme N, Hebblen D. 2011. Reconstructing the thermal structure of the upper ocean: insights from planktic foraminifera shell chemistry and alkenones in modern sediments of the tropical eastern Indian Ocean. *Paleoceanography* 26: PA3219, doi: 10.1029/2011PA002132.

Newcomb KR, McGann WR. 1987. Seismic history and seismotectonics of the Sunda Arc. *Journal of Geophysical Research* 92(B1):421–39.

Newton A, Thunell R, Stott A. 2006. Climate and hydrographic variability in the Indo-Pacific Warm Pool during the last millennium. *Geophysical Research Letters* 33: L19710, doi:10.1029/2006GL027234.

Oppo D, Rosenthal Y, Linsley BK. 2009. 2,000-year-long temperature and hydrology reconstructions from the Indo-Pacific warm pool. *Nature* 460(7259):1113–6.

Ortlieb L, Vargas G, Saliège J-F. 2011. Marine radiocarbon reservoir effect along the northern Chile-southern Peru coast (14–24°S) throughout the Holocene. *Quaternary Research* 75(1):91–103.

Reimer PJ, Baillie MGL, Bard E, Bayliss A, Beck JW, Blackwell PG, Bronk Ramsey C, Buck CE, Burr GS, Edwards RL, Friedrich M, Grootes PM, Guilderson TP, Hajdas I, Heaton T, Hogg AG, Hughen KA, Kaiser KF, Kromer B, McCormac FG, Manning SW, Reimer RW, Richards DA, Southon JR, Talamo S, Turney CSM, van der Plicht J, Weyhenmeyer CE. 2009. IntCal09 and Marine09 radiocarbon age calibration curves, 0–50,000 years cal BP. *Radiocarbon* 51(4): 1111–50.

Schmidt DN, Elliott T, Kasemann SA. 2008. The influences of growth rates on planktic foraminfers as proxies for paleostudies – a review. In: Austin WEN, James RH, editors. *Biogeochemical Controls on Paleoceanographic Environmental Proxies*. Geological Society Special Publication 303. Wiltshire: Cromwell Press. p 73–86.

Self S, Rampino MR, Newton MS, Wolff JA. 1984. Volcanological study of the great Tambora eruption of 1815. *Geology* 12(11):659–63.

Simkin T, Siebert L. 1994. *Volcanoes of the World*. 2nd edition. Tucson: Geoscience Press. 369 p.

Sprintall J, Potemra JT, Hautala SL, Bray NA, Pandoe WW. 2003. Temperature and salinity variability in the exit passages of the Indonesian Throughflow. *Deep-Sea Research II* 50(12):2183–204.

Stothers RB. 1984. Mystery cloud of AD 536. *Nature* 307(5949):344–5.

Susanto RD, Gordon RL, Zheng Q. 2001. Upwelling along the coasts of Java and Sumatra and its relation to ENSO. *Geophysical Research Letters* 28(8):1599–602.

Verbeek R. 1885. *Krakatau*. Batavia: State Press. 495 p.

Whitten T, Soeriaatmadji RE, Afiff SA. 1996. *The Ecology of Indonesia Series II: The Ecology of Java and Bali*. Hong Kong: Periplus Editions. 1009 p.

Wjiffels S, Bray N, Hautala S, Meyers G, Morawitz G. 1996. The WOCE Indonesian Throughflow repeat hydrography sections: 110 and 1R6. *WOCE Newsletter* 24:25–8.

Wohletz K. 2000. Were the Dark Ages triggered by volcano-related climate changes in the 6th century? [abstract]. *EOS* 81(48): F1305.